

# Spin-dependent tunneling in nanostructures consisting of magnetic barriers

Maowang Lu<sup>1,a</sup>, Lide Zhang<sup>1</sup>, Yunxia Jin<sup>1</sup>, and Xiaohong Yan<sup>1,2</sup>

<sup>1</sup> Institute of Solid State Physics, Chinese Academy of Sciences, PO Box 1129, Hefei 230031, PR China

<sup>2</sup> Department of Physics, Xiangtan University, Xiangtan, Hunan 411105, PR China

Received 27 December 2001 and Received in final form 13 March 2002

Published online 25 June 2002 – © EDP Sciences, Società Italiana di Fisica, Springer-Verlag 2002

**Abstract.** We study the spin-dependent transport properties of the nanostructures consisting of realistic magnetic barriers produced by the deposition of ferromagnetic stripes on heterostructures. It is shown that, only in the nanostructures with symmetric magnetic field with respect to the magnetic-modulation direction, electrons exhibit a considerable spin-polarization. It is also shown that the degree of the electron spin polarization is greatly dependent on the ferromagnetic stripe and its position relative to the 2DEG. A much larger electron-spin polarization can be obtained by properly fabricating the ferromagnetic stripe and by adjusting its distance above the 2DEG.

**PACS.** 73.40.Gk Tunneling – 72.10.-d Theory of electronic transport; scattering mechanisms – 73.23.-b Electronic transport in mesoscopic systems – 75.70.Cn Interfacial magnetic properties (multilayers, superlattices)

## Nomenclature

2DEG	two-dimensional electron gas
$q$	wave vector in $y$ direction
$\sigma$	electron spin
$\mu_B$	Bohr magneton
$m^*$	effective mass of electron
$g^*$	effective Landè factor of electron
$B$	magnetic field
$M_0$	magnetisation of the stripe
$h$	height of the strip
$d$	thickness of the stripe
$z_0$	distance of the stripe to 2DEG
$x, y, z$	coordinates
$A(x)$	magnetic vector potential
$V_\sigma(x, q)$	effective potential of structure
$l_B$	magnetic length
$\omega_c$	cyclotron frequency
$E$	electronic energy
$x_-(x_+)$	left (right) end of magnetic barrier
$T_\sigma(E, q)$	transmission coefficient
$P_T(E, q)$	electron-spin polarization
$E_F$	Fermi energy
$G_\sigma(E_F)$	ballistic conductance
$P_G(E_F)$	spin-conductance polarization
$v_F$	Fermi velocity

In the recent years, spin-polarized transport in nanostructures has attracted considerable attention due to its importance in both basic research and practical application [1–6]. The increasing interest in this topic stems from two major factors. The first one is that advances in semiconductor microfabrications have made it feasible to produce structures which possess electrical properties greatly sensitive to electron spin. So-called “spintronics” devices can be controlled by the electron spin polarization. The second factor is that one can exploit a quite general physical approach to clarify unusual spin-dependent phenomena in low-dimensional structures.

Magnetic-barrier nanostructures are relevant to the new class of semiconductor quantum structures, which can be experimentally realized by the deposition of a two-dimensional electron gas (2DEG) in an inhomogeneous magnetic field [7]. There have been numerous studies, both experimental and theoretical, devoted to the transport properties of magnetic-barrier nanostructures [7–12]. However, in these studies the interaction of the electronic spin with the magnetic-barrier field has been overlooked. Recently, a few articles have called attention to some peculiarities in the dependence of the tunneling probability and the conductance on the electronic spin [13–15]. Using a simple  $\delta$ -function magnetic-barrier, effects of intrinsic spin on electronic transport properties were first investigated by Majumdar [13]. It was found that the interaction of the intrinsic spin of 2DEG with the magnetic field significantly changes the tunneling

<sup>a</sup> e-mail: yxjin@mail.issp.ac.cn

probability and the conductance of electrons through magnetic barriers. Subsequently, the spin- and wave-vector dependent resonant tunneling of electrons through rectangular and sawtooth magnetic-barriers have also been studied [14]. Very recently, the spin-dependent electron tunneling through rectangular magnetic-barriers has been investigated with and without an external electric field in reference [15]. It was found that only in the asymmetric rectangular magnetic barriers electrons exhibit a considerable spin-polarization, and that the external electric field can greatly change the spin polarization of electrons. However, all the magnetic barriers used in these studies are not the *realistic* ones. For the realistic magnetic barrier structures, electronic transport properties have been studied by our group headed by Lide Zhang [8], but we did not consider still the effect of electron-spin. Therefore, in order to reveal the spin-dependent transport properties of realistic magnetic nanostructures, in this paper we study the realistic magnetic barriers instead of the ideal ones. The general rule of the spin polarization for electron tunneling through the realistic magnetic barriers is found. We also discuss the effect of parameters of the system on the magnitude of the electron-spin polarization.

As an illustrative example, we consider two types of realistic magnetic barriers, which is produced by the deposition, on the surface of a heterostructure, of a ferromagnetic stripe with magnetization (a) perpendicular and (b) parallel to the 2DEG located at a distance  $z_0$  below the stripe (see the schematic illustration of the system on the top of Fig. 1). For these two structures, the magnetic barriers experienced by the 2DEG are given by [7]

$$\mathbf{B} = B(x)\hat{z}$$

$$B(x) = (M_0h) [f(x + d/2) - f(x - d/2)], \quad (1)$$

where (a)  $f(x) = 2x/(x^2 + z_0^2)$ , and (b)  $f(x) = -z_0/(x^2 + z_0^2)$ .  $M_0$ ,  $d$ , and  $h$  are the magnetization, thickness, and height of the ferromagnetic stripe. The two magnetic barriers are shown in Figures 1a and b, respectively, where the structural parameters are both chosen to be  $M_0h = 1.0$ ,  $d = 1.0$ , and  $z_0 = 0.1$ ; the left and right ends of magnetic barriers are located at  $x_- = -1.5$  and  $x_+ = +1.5$ .

The Hamiltonian for the 2DEG system assumed in the  $xy$  plane with the consideration of the electron spin can be written as

$$H = \frac{1}{2m^*} [\mathbf{P} + e\mathbf{A}(x)]^2 + \frac{1}{2}\sigma\mu_B g^* B(x), \quad (2)$$

where  $\mu_B = e\hbar/2m^*$  is the Bohr magneton,  $m^*$  is the effective mass of electron,  $\mathbf{P}$  is the momentum of the electron,  $g^*$  is the effective Landé factor of the electron in a real 2DEG realized using semiconductor,  $\sigma = +1/-1$  for the up/down spin directions, and  $\mathbf{A}(x) = [0, A(x), 0]$  is the magnetic vector potential given, in Landau gauge, by  $A(x) = (M_0h) \ln \left[ \frac{(x+d/2)^2 + z_0^2}{(x-d/2)^2 + z_0^2} \right]$ , and  $A(x) = (M_0h) \left[ \tan^{-1} \left( \frac{x-d/2}{z_0} \right) - \tan^{-1} \left( \frac{x+d/2}{z_0} \right) \right]$  for magnetic barriers (a) and (b), respectively. It is convenient to express quantities in dimensionless units by

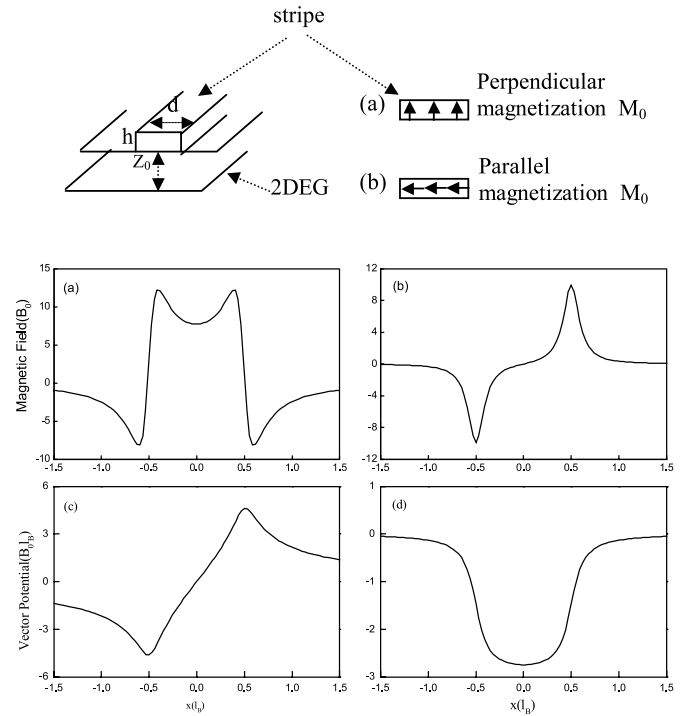


**Fig. 1.** Magnetic barriers and the corresponding vector potentials, where schematic illustration of the system is placed on the top and the structural parameters are chosen to  $M_0h = 1.0$ ,  $d = 1.0$ , and  $z_0 = 0.1$ . The left and right ends of the barriers are located at  $x_- = -1.5$  and  $x_+ = 1.5$ , respectively.

using the cyclotron frequency  $\omega_c = eB_0/m^*$  and the magnetic length  $l_B = \sqrt{\hbar/eB_0}$ . For GaAs,  $g^* = 0.44$ ,  $m^* = 0.067m_e$  with  $m_e$  being the free-electron mass, and an estimated  $B_0 = 0.1$  T, we obtain  $l_B = 813$  Å and  $\hbar\omega_c = 0.17$  meV. The relevant quantities can be expressed in dimensionless units: (1) the coordinate  $x \rightarrow l_B x$ , (2) the magnetic field  $B(x) \rightarrow B_0 B(x)$ , (3) the vector potential  $A(x) \rightarrow B_0 l_B A(x)$ , and (4) the energy  $E \rightarrow \hbar\omega_c E$ .

The two-dimensional Schrödinger equation  $H\Psi(x, y) = E\Psi(x, y)$  with  $H$  given by equation (2) in the dimensionless units has solutions of the form  $\Psi(x, y) = e^{iqy}\psi(x)$ , where  $E$  is the total energy of the electron and  $q$  is the electron wave vector in the  $y$  direction. The wave function  $\psi(x)$  satisfies the following 1D Schrödinger equation

$$\left\{ \frac{d^2}{dx^2} - [A(x) + q]^2 + g^*\sigma B(x)/2 \right\} \psi(x) = 2E\psi(x), \quad (3)$$

where  $V_\sigma(x, q) = [A(x) + q]^2 + g^*\sigma B(x)/2$  is the effective potential of the corresponding structure, which depends clearly upon the magnetic configuration  $B(x)$ , the  $y$ -directed wave vector  $q$ , and the electron spin  $\sigma$ . For a MB structure with a complex effective potential  $V_\sigma(x, q)$  within the region  $[x_-, x_+]$ , it is difficult to directly solve equation (3). Here we follow the spirit of the well-established method in reference [8]. For that we divide the region into  $N(\gg 1)$  segments, each of which has width  $a = (x_+ - x_-)/N$ , and treat the

effective potential as a constant  $V_\sigma = [x_- + (j-1)a, q]$  in the  $j$ th segment  $[x_- + (j-1)a, x_- + ja]$ . Within this segment, the Schrödinger equation (3) then becomes  $\left\{ \frac{d^2}{dx^2} - V_\sigma [x_- + (j-1)a, q] + 2E \right\} \psi(x) = 0$ , which has the plane-wave solution,  $\psi_j(x) = c_j e^{ik_j x} + d_j e^{-ik_j x}$ , where  $k_j = \{2E - V_\sigma [x_- + (j-1)a, q]\}^{1/2}$ . Without any loss of generality, in both incident and outgoing regions of the magnetic barrier, the wave functions can be assumed as  $\psi(x) = e^{ikx} + r e^{-ikx}$ ,  $x < x_-$ , and  $t e^{ikx}$ ,  $x > x_+$ , respectively, where  $k = \sqrt{2E - q^2}$ ,  $r$  is the reflection amplitude, and  $t$  is transmission amplitude. From the wave-function-matching conditions at the boundaries of the segments and at  $x = x_-, x_+$ , we obtain

$$\begin{pmatrix} e^{ikx_-} & e^{-ikx_-} \\ ike^{ikx_-} & -ike^{-ikx_-} \end{pmatrix} \begin{pmatrix} 1 \\ r \end{pmatrix} = M \begin{pmatrix} e^{ikx_+} & e^{-ikx_+} \\ ike^{ikx_+} & -ike^{-ikx_+} \end{pmatrix} \begin{pmatrix} t \\ 0 \end{pmatrix} \quad (4)$$

where

$$M = \begin{pmatrix} M_{11} & M_{12} \\ M_{21} & M_{22} \end{pmatrix} = \prod_{j=1}^N M_j$$

and

$$M_j = \begin{pmatrix} \cos(k_j a) & -\sin(k_j a)/k_j \\ k_j \sin(k_j a) & \cos(k_j a) \end{pmatrix}$$

are the transfer matrix and the  $j$ th transfer matrix for the  $j$ th segment, respectively. Therefore, the spin-dependent transmission coefficient for electron tunneling through the MB nanostructure within the region  $[x_-, x_+]$  can be easily obtained from the transfer matrix  $M$

$$T_\sigma(E, q) = 4 \left| (M_{11} + M_{22}) + i \left( k M_{12} - \frac{M_{21}}{k} \right) \right|^{-2}. \quad (5)$$

To evaluate the electron spin-polarization effect in the tunneling process, one usually calculates the spin polarization of the transmitted beam defined in terms of the spin-dependent transmission coefficient  $T_\sigma(E, q)$  and given by

$$P_T(E, q) = \frac{T_+(E, q) - T_-(E, q)}{T_+(E, q) + T_-(E, q)}, \quad (6)$$

where  $T_+$  and  $T_-$  are transmission coefficients for spin-up and spin-down electrons, respectively. Using the transmission coefficient  $T_\sigma(E, q)$ , the spin-dependent conductance of the electrons tunneling through the magnetic barrier structures can be calculated in the ballistic regime as the average electron flow over half the Fermi surface from the well-known Landau-Büttiker formula and is given by [7]

$$G_\sigma(E_F) = G_0 \int_{-\pi/2}^{\pi/2} T_\sigma(E_F, \sqrt{2E_F} \sin \theta) \cos \theta d\theta, \quad (7)$$

where  $E_F$  is the Fermi energy and  $\theta$  is the angle between the direction of the incident electron and the  $x$  direction.  $G_0 = e^2 m^* \nu_F L_y / (2\hbar^2)$ , where  $L_y$  is the length of the

structure in the  $y$  direction and  $\nu_F$  is the Fermi velocity. Similar to the spin polarization  $P_T$ , we also introduce spin-conductance polarization  $P_G$  of the magnetic nanostructure defined by

$$P_G(E_F) = \frac{G_+(E_F) - G_-(E_F)}{G_+(E_F) + G_-(E_F)}, \quad (8)$$

where  $G_+$  and  $G_-$  correspond conductances of up- and down- spin electrons, respectively.

Here, we would like to point out several points on our theory depicted above. In the present work, we consider ballistic transport of high mobility two-dimensional electron gases (2DEG) with mean free path not less than dimension of magnetic structure in tunneling direction in low temperature. Our approximation method described above is reliable, since it follows the spirit of numerical method in reference [8], which is demonstrated to be accurate enough (see Fig. 2 in Ref. [8]). In this paper, we restrict our calculations to a single realistic magnetic barrier, but our calculated method can also be applied to more complicated multiple-barriers magnetic structures, even magnetic superlattices, where the calculations will be too time-consuming. In addition, the reality of the realistic magnetic barriers means that the magnetic field is obtained by directly integrating Maxwell's equations for the system (see Ref. [7]) and its magnetic profile is not ideal such as rectangular or sawtooth.

First of all, to demonstrate the effect of electron spin on the transmission, we have calculated transmission coefficients of  $T_0$  (without spin),  $T_+$  (up-spin), and  $T_-$  (down-spin) for electrons tunneling through realistic magnetic barriers. Figure 2 shows these transmission coefficients as functions of the energy  $E$  and the wave vector  $q$  for the magnetic barrier as shown in Figure 1a, where the structural parameters are chosen to be  $M_0 \hbar = 1.0$ ,  $d = 1.0$ , and  $z_0 = 0.1$ . It is evident that both  $T_+$  and  $T_-$  differ from  $T_0$ , especially in low energy region, *i.e.*, the interaction of the electron spin with the magnetic field significantly changes the tunneling probability of electrons through magnetic barriers. This is a consequence of the variation of the effective potential  $V_\sigma(x, q)$  due to the interaction of the electronic spin with the magnetic field. Also, one can clearly see that the transmission coefficient  $T_+$  of up-spin electrons is greatly different from the transmission coefficient  $T_-$  of down-spin electrons. Curve  $T_+$  shifts toward high-energy region, while  $T_-$  does toward the opposite direction, and thus spin splitting of transmission probability or the dependence of transmission probability on the electron spin directions appears. This occurs because for this magnetic barrier the magnetic field  $B(x)$  and the corresponding vector potential  $A(x)$  are symmetric and antisymmetric with respect to  $x$ , respectively. As a consequence of this,  $V_+(x, q) \equiv [A(x) + q]^2 + g^* B_z(x)/2 \neq V_-(x, q) \equiv [A(x) + q]^2 - g^* B_z(x)/2$  according to the well-known fact that the transmission coefficient through a potential barrier is equal for particles moving in opposite directions (*i.e.*, the tunneling characteristics are invariant with respect to the replacement  $x \rightarrow -x$  in the equation of motion), leads to the dependence of the

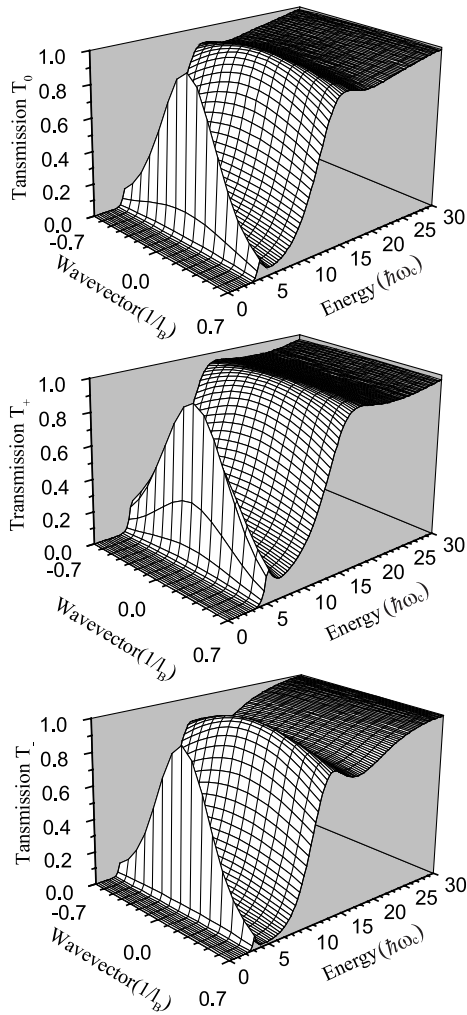


**Fig. 2.** Transmission coefficients of  $T_0$  (without-spin),  $T_+$  (up-spin), and  $T_-$  (down-spin) for electrons tunneling through the magnetic barrier presented in Figure 1a.

transmission coefficient on the spin directions. In addition, it is interesting to note that the transmission coefficient ( $T_0$ ,  $T_+$ , or  $T_-$ ) is symmetric about the  $q = 0$  plane also for the same reason. As for the magnetic barrier shown in Figure 1b, because its magnetic field  $B(x)$  is antisymmetric and vector potential  $A(x)$  is symmetric relative to the  $x$ ,  $V_+(x, q) = V_-(x, q)$  leads to  $T_+ = T_-$ , *i.e.*, in this kind of magnetic barrier transmission coefficient of electron is independent of the spin direction [16]. Moreover, the transmission coefficient ( $T_0$ ,  $T_+$ , or  $T_-$ ) is antisymmetric about the  $q = 0$  plane, nevertheless  $T_+$ , or  $T_-$  is still different from  $T_0$ .

If there exists a difference of transmission coefficient between up-spin and down-spin electrons, namely,  $T_+ \neq T_-$ , the electrons in the tunneling process will show up spin polarization effect, *i.e.*,  $P_T \neq 0$ . Accordingly, for the magnetic barrier shown in Figure 1a the electrons should show up a rather evident spin polarization due to

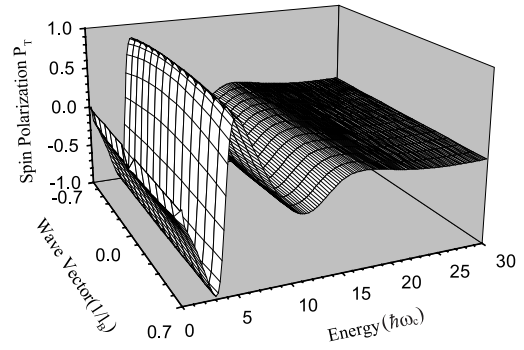


**Fig. 3.** The spin polarization for electron tunneling through the magnetic barrier given in Figure 1a with structural parameters  $M_0h = 1.0$ ,  $d = 1.0$ , and  $z_0 = 0.1$ .

the significant difference between up-spin and down-spin transmissions ( $T_+$  and  $T_-$ ), while the magnetic barrier shown in Figure 1b does not. In Figure 3 we present the electron spin polarization  $P_T$  through the magnetic barrier of Figure 1a, as a function of the energy  $E$  and the wave vector  $q$ , where the structural parameters are chosen to be the same as in Figure 2. The considerable electron spin-polarization is clearly seen. Moreover, the spin polarization is strongly dependent on electronic energy  $E$ . For small electronic energy, the electron shows up very strong spin polarization, while for large electronic energy, the spin polarization is weakened, and finally approaches zero. But the spin polarization is slightly associated with the electron wave vector  $q$  in the  $y$  direction. Furthermore, from the definition of the electron spin polarization (*cf.* Eq. (6)), one can easily find  $P_T$  is symmetric about the  $q = 0$  plane since both transmission coefficients  $T_+$  and  $T_-$  are symmetric with respect to the  $q = 0$  plane. For the magnetic barrier given in Figure 1b, the transmission coefficient  $T_+ = T_-$  and therefore this type of magnetic barrier structure does not show up spin polarization. So far, we can conclude from the above results that for the realistic magnetic barriers proposed by Matulis *et al.* [7], only magnetic nanostructures with symmetric magnetic fields about the  $x$  axis show up a considerable spin polarization effect. And, the magnitude of the spin polarization is dependent greatly upon the electronic energy  $E$  and weakly upon the transverse wave vector  $q$  of the electron.

We then examine the electron spin effect on the conductance through the magnetic barrier shown in Figure 1a. Figure 4 shows the results that the conductance *versus* Fermi energy, where the parameters are the same as in Figure 3, the conductance is normalized with respect to  $G_0$ , and the spin-conductance polarization  $P_G$  is given in the inset. Here, the solid, dashed, and dotted curves correspond to without spin, up-spin, and down-spin electrons, respectively. Despite the averaging of  $T_\sigma(E, q)$  over half the Fermi surface, the main feature of the electron transmission is still reflected in the conductance. From this figure one can clearly see that spin-conductance (dashed or dotted curve) and without-spin conductance (solid

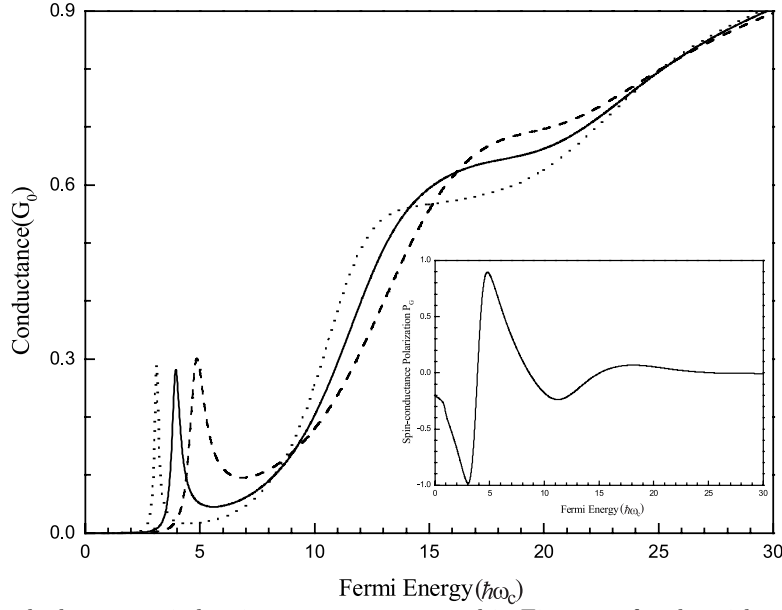


**Fig. 4.** Conductance through the magnetic-barrier structure presented in Figure 1a for the without-spin (solid curve), up-spin (dashed curve), and down-spin (dotted curve), where the conductance is in units of  $G_0$ . The corresponding spin-conductance polarization is shown in the inset.

curve) are very different. Also, we can see that up-spin conductance (dashed curve) is greatly different from that of down-spin (dotted curve), where dashed curve shifts toward high-energy end, while dotted curve does toward low-energy direction. Because there is a significant difference in the conductance between up- and down-spin electrons (*i.e.*, the conductance depends strongly on the direction of the electron spin), the magnetic barrier structure exhibits an evident spin-conductance polarization effect as depicted in the inset of Figure 4, especially in low Fermi energy. For large Fermi energy, the spin-conductance polarization  $P_G$  is weakened, and finally approaches zero. Two sharp peaks in  $P_G$  curve in low-energy region correspond to two low-energy resonant peaks of spin conductance curves ( $G_+$  and  $G_-$ ), respectively. These features are similar to those of the spin polarization  $P_T$  as given in Figure 3.

Finally, we study the effect of the ferromagnetic stripe and its position relative to the 2DEG on the electron spin polarization for the magnetic barrier shown in Figure 1a. Figures 5a–c show the spin polarization  $P_T$  as a function of the energy  $E$  and the wave vector  $q$ , for the different structural parameters of ferromagnetic stripe and  $z_0$ : (a)  $M_0h = 1.0$ ,  $d = 1.0$ , and  $z_0 = 0.3$ ; (b)  $M_0h = 1.5$ ,  $d = 1.0$  and  $z_0 = 0.1$ ; and (c)  $M_0h = 1.0$ ,  $d = 1.5$ , and  $z_0 = 0.1$ , respectively. In contrast to the Figure 3 that is for the structural parameters of  $M_0h = 1.0$ ,  $d = 1.0$ , and  $z = 0.1$ , it is apparent from these figures that the ferromagnetic stripe and the distance  $z_0$  strongly influence the magnitude of the spin polarization. The spin polarization  $P_T$  is weakened with the  $z_0$  increasing and occurs in much less electronic energy range approaching low energy region. When the  $M_0h$  increases,  $P_T$  is enhanced and is extended. The spin polarization  $P_T$  is enhanced, and exhibits more and sharper peaks, with the  $d$  increasing.

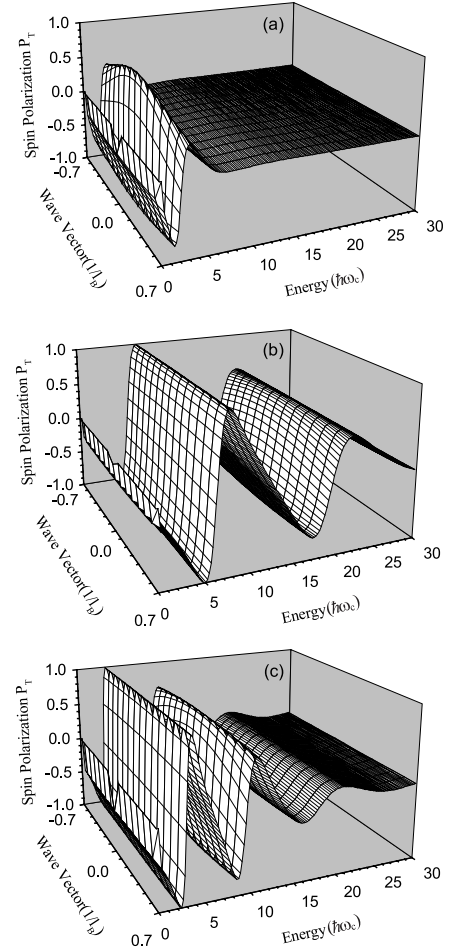


**Fig. 5.** The electron spin polarization for the magnetic barrier presented in Figure 1a with the different structural parameters (a)  $M_0h = 1.0$ ,  $d = 1.0$ ,  $z_0 = 0.3$ , (b)  $M_0h = 1.5$ ,  $d = 1.0$ ,  $z_0 = 0.1$ , and (c)  $M_0h = 1.0$ ,  $d = 1.5$ ,  $z_0 = 0.1$ , respectively.

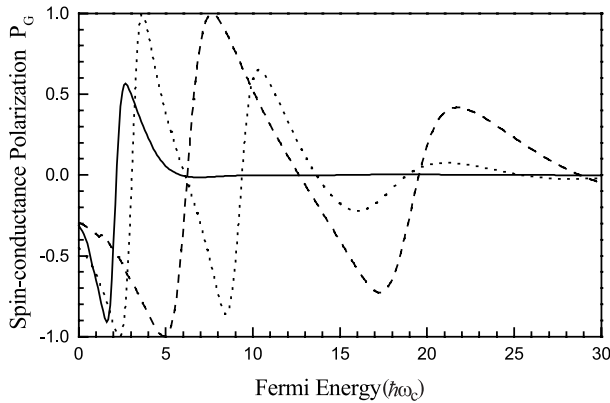


**Fig. 6.** The spin-conductance polarization for the magnetic barrier presented in Figure 1a, where the solid, dashed, and dotted curves correspond to the structural parameters ( $M_0h = 1.0$ ,  $d = 1.0$ ,  $z_0 = 0.3$ ), ( $M_0h = 1.5$ ,  $d = 1.0$ ,  $z_0 = 0.1$ ), and ( $M_0h = 1.0$ ,  $d = 1.5$ ,  $z_0 = 0.1$ ), respectively.

Similar features are also reflected in spin-conductance polarization  $P_G$  as given in Figure 6, where the solid, dashed, and dotted curves correspond to the cases (a), (b) and (c) in Figure 5, respectively. All these features of the ferromagnetic stripe and  $z_0$  effect on the electron spin polarization ( $P_T$  and  $P_G$ ) are due to the change of the effective potential  $V_\sigma(x, q)$  via the magnetic field  $B(x)$  when the parameters of the system are altered. These features also hint that a much larger spin polarization or much better spin-filtering properties for magnetic barriers can be obtained by both using the proper ferromagnetic stripe and adjusting the distance  $z_0$ , which may be useful for fabrication of spin devices based on such magnetic barriers.

In conclusion, we have studied electronic spin-dependent transport in the realistic magnetic-barrier nanostructure proposed by Matulis *et al.* [7], which can be experimentally realized by the deposition of ferromagnetic stripes on heterostructures. We have shown that, for the structures with symmetric magnetic field about the  $x$  axis (magnetic modulation direction), the transmission of 2DEG depends greatly on the spin direction. Thus, this type of realistic magnetic barrier is found to possess a considerable spin polarization effect, which is dependent strongly upon the incident electron energy, and poorly upon the incident electron wave vector. We have also exhibited that the magnitude of this electron spin polarization is greatly influenced by the ferromagnetic stripe

and its distance to 2DEG. Therefore, a much larger spin polarization can be obtained by properly fabricating the ferromagnetic stripes and by adjusting their locations relative to the 2DEG.

The authors would like to acknowledge support by National Major project of Fundamental Research: Ministry of Sciences and Technology of China under Grant No. 1999064501 and by the National Natural Science Foundation of China under Grant No. 10074064.

## References

1. G.A. Prinz, Science **282**, 1660 (1998); Phys. Today **48**, 58 (1995)
2. B.E. Kane, Nature (London) **393**, 133 (1998)
3. N.N. Kuzma, P. Khandelwal, S.E. Barrett, L.N. Pfeiffer, K.W. West, Science **281**, 686 (1998); P. Khandelwal, N.N. Kuzma, S.E. Barrett, L.N. Pfeiffer, K.W. West, Phys. Rev. Lett. **81**, 673 (1998)
4. L. Balents, R. Egger, Phys. Rev. Lett. **85**, 3464 (2000)
5. P. Šeba, P. Exner, K.N. Pichugin, A. Vyhnal, P. Středa, Phys. Rev. Lett. **86**, 1598 (2001)
6. A. Voskoboynikov, C.P. Lee, O. Tretyak, Phys. Rev. B **63**, 165306 (2001)
7. A. Matulis, F.M. Peeters, P. Vasilopoulos, Phys. Rev. Lett. **72**, 1518 (1994)
8. J.Q. You, Lide Zhang, P.K. Ghosh, Phys. Rev. B **52**, 17243 (1995)
9. Y. Guo, B.L. Gu, Z.Q. Li, Q. Sun, Y. Kawazoe, Eur. Phys. J. B **3**, 257 (1998); *ibid.* **3**, 263 (1998)
10. F.M. Peeters, X.Q. Li, Appl. Phys. Lett. **72**, 512 (1998)
11. A. Matulis, F.M. Peeters, Phys. Rev. B **62**, 91 (2000)
12. A. Nogret, S.J. Bending, Phys. Rev. Lett. **84**, 2231 (2000)
13. A. Majumdar, Phys. Rev. B **54**, 11911 (1996)
14. V.N. Dobrovosky, D.I. Sheka, B.V. Chemyachuk, Surf. Sci. **397**, 333 (1998)
15. Yong Guo, Bing-Lin Gu, Zhong Zeng, Jing-Zhi Yu, Yoshiyuki Kawazoe, Phys. Rev. B **62**, 2635 (2000)
16. We have also calculated the transmission coefficients  $T_0$  (without spin),  $T_+$  (up-spin), and  $T_-$  (down-spin) for electrons tunneling through the magnetic barrier presented in Figure 1b. The results show that the  $T_+$  or  $T_-$  is different from  $T_0$ , but  $T_+$  equals to  $T_-$